On Martin Disteli's Main Achievements in Spatial Gearing: Disteli's Diagram

Giorgio Figliolini[*]   Hellmuth Stachel[†]   Jorge Angeles[‡]

The subject of this paper is a diagram due to Martin Disteli. The diagram, illustrating the relation between the angular velocities of a pair of skew gears, is intended for the analysis of the relative screw motion between the two gears. The diagram, based on a circle, seems to have been overlooked by the community of kinematicians.

Introduction

Martin Disteli[1] transferred Releaux's principle of gearing for the particular case of cycloid gears from the sphere into three-dimensional space — cf. Disteli (1904) and Disteli (1911). This transfer led to the analysis of a pair of meshing skew gears whose tooth flanks are ruled surfaces, in contact along lines. Disteli (1911) produced a simple diagram illustrating the relation between the angular velocities of a pair of skew gears and the position and pitch of their relative screw motion. The latter will be addressed in this note, while both items seem to have been overlooked by the community of kinematicians.

Disteli's papers are hard to read because of a) their lack of vector notation, which leads to lengthy expressions from where little information can be drawn and b) the use of rather uncommon left-hand frames. Although Disteli used screw theory, he described screws only explicitly, by listing their six coordinates (p, q, r, u, v, w). Moreover, the up-to-six different frames occurring in the paper are not identified by subscripts, but rather by different characters. These shortcomings of Disteli's publications were mentioned in his obituary, Schur (1927). We follow the final comment in this obituary, which reads: *"It would be desirable that somebody rewrites Disteli's arguments, thus making them much more understandable"*.

We try to meet this target by a consistent use of dual vectors representing directed lines and screws — cf., e.g., Müller (1963); Veldkamp (1976); Angeles (1998); McCarthy (2000); Stachel (2005). In the sequel we identify oriented lines g with their dual unit vectors $\widehat{\mathbf{g}}$, thus speaking

[*]Dipartimento di Meccanica, Stutture, Ambiente e Territorio, University of Cassino, figliolini@unicas.it

[†]Institute of Discrete Mathematics and Geometry, Vienna University of Technology, stachel@dmg.tuwien.ac.at

[‡]Dept. of Mechanical Engineering & CIM, McGill University, Montreal, angeles@cim.mcgill.ca

[1] Martin Disteli (1862–1923) was Professor of geometry at the technical universities of Dresden and Karlsruhe.

briefly of *"the line $\widehat{\mathbf{g}}$"* instead of the directed line g with its dual vector $\widehat{\mathbf{g}}$ — see, e.g., Husty et al. (1997) or Stachel (2005). In the same way *"the screw $\widehat{\mathbf{q}}_{ij}$"* stands for the instant screw of the relative motion between the two frames Σ_i and Σ_j, this screw being represented by the dual vector $\widehat{\mathbf{q}}_{ij} = \widehat{\omega}_{ij}\,\widehat{\mathbf{p}}_{ij}$. Here, $\widehat{\mathbf{p}}_{ij}$ is the screw axis and $\widehat{\omega}_{ij} = \omega_{ij} + \varepsilon\omega_{0ij}$ is the dual *amplitude* of the twist, with *signed magnitudes* of the angular velocity and the point velocity along the screw axis ω_{ij} and ω_{0ij}, respectively.
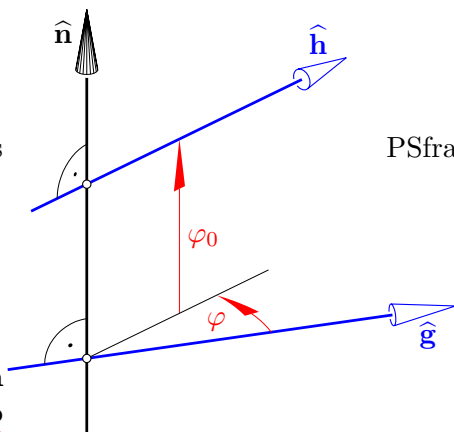

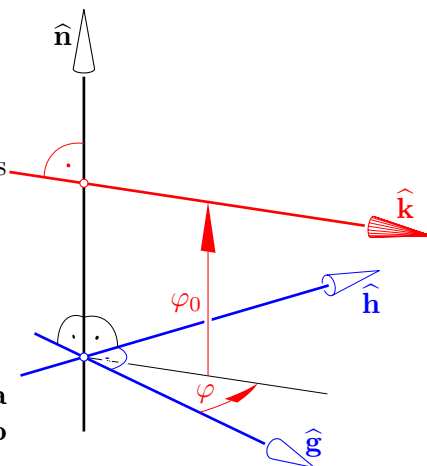Figure 1: Dual angle $\widehat{\varphi} = \varphi + \varepsilon\varphi_0$

Figure 2: $\widehat{\mathbf{k}} = \cos\widehat{\varphi}\,\widehat{\mathbf{g}} + \sin\widehat{\varphi}\,\widehat{\mathbf{h}}$

We recall below some standard formulas pertaining to dual unit vectors — cf. Angeles (1998) — which will be used presently.

a) For two given directed lines $\widehat{\mathbf{g}}$, $\widehat{\mathbf{h}}$, let $\widehat{\mathbf{n}}$ denote the common normal, given by $\mathbf{n} \equiv \mathbf{g} \times \mathbf{h}$. If the helical motion along $\widehat{\mathbf{n}}$, which transforms $\widehat{\mathbf{g}}$ into $\widehat{\mathbf{h}}$ — see Fig. 1 — entails the angle φ of rotation and the translation φ_0, and we combine them in the dual angle $\widehat{\varphi} \equiv \varphi + \varepsilon\varphi_0$, then,

$$
\begin{aligned}
\widehat{\mathbf{g}}\cdot\widehat{\mathbf{h}} &= \mathbf{g}\cdot\mathbf{h} + \varepsilon(\mathbf{g}_0\cdot\mathbf{h} + \mathbf{g}\cdot\mathbf{h}_0) &&= \cos\widehat{\varphi} &&= \cos\varphi - \varepsilon\varphi_0\sin\varphi \quad \text{and}\\
\widehat{\mathbf{g}}\times\widehat{\mathbf{h}} &= \mathbf{g}\times\mathbf{h} + \varepsilon(\mathbf{g}_0\times\mathbf{h} + \mathbf{g}\times\mathbf{h}_0) &&= \sin\widehat{\varphi}\,\widehat{\mathbf{n}} &&= \sin\varphi\,\mathbf{n} + \varepsilon\left[\sin\varphi\,\mathbf{n}_0 + \varphi_0\cos\varphi\,\mathbf{n}\right].
\end{aligned}
\tag{1}
$$

Further, we recall the dual extension of differentiable functions, defined as

$$
f(\widehat{x}) = f(x + \varepsilon x_0) = f(x) + \varepsilon\,x_0 f'(x).
$$

which involves the first two terms of the Taylor series of $f(\,\cdot\,)$ at a value $x + \varepsilon x_0$ of its argument, where due to a property of the dual unit, $\varepsilon^2 = 0$, all higher-order terms vanish. This guarantees that identities like $\cos^2 x + \sin^2 x = 1$ are preserved under the dual extension, as they are valid for the power series too.

The notation ε stems from the observation that the dual unit can be regarded as such a small number that its square is negligible. Note that only dual numbers $\widehat{x} = x + \varepsilon x_0$ with non-vanishing primal part, i.e., with $x \neq 0$, have an inverse $\widehat{x}^{-1} = \frac{1}{x}(x - \varepsilon x_0)$; inverses of *pure* dual numbers, i.e., those with $x = 0$, bear zero divisors. Dual numbers were first introduced by Clifford (1873) = (Clifford, 1882, pp. 181–200).

b) Let $\widehat{\mathbf{g}}$ and $\widehat{\mathbf{h}}$ be two spears intersecting at right angles, their common perpendicular being $\widehat{\mathbf{n}}$. Then,

$$
\widehat{\mathbf{k}} = \cos\widehat{\varphi}\,\widehat{\mathbf{g}} + \sin\widehat{\varphi}\,\widehat{\mathbf{h}}
\tag{2}
$$

is the image of $\widehat{\mathbf{g}}$ under the helical motion along $\widehat{\mathbf{n}}$ through the dual angle $\widehat{\varphi}$ — see Fig. 2.
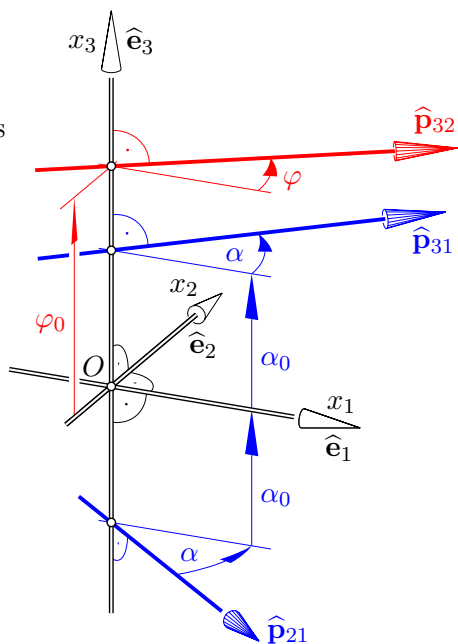
1 Disteli's Diagram: Pure Rotations

g replacements

Figure 3: Axes $\widehat{\mathbf{p}}_{21}$, $\widehat{\mathbf{p}}_{31}$ of the pinion and the gear wheels, and the relative axis $\widehat{\mathbf{p}}_{32}$
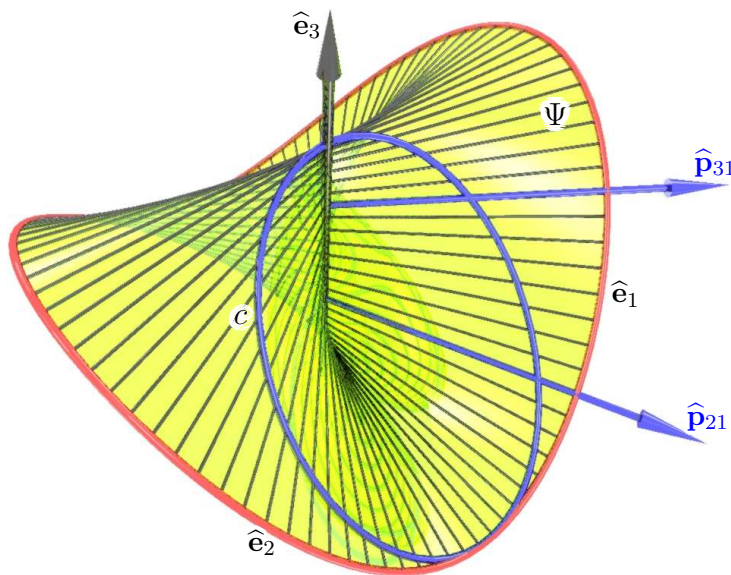

Figure 4: Plücker's conoid = cylindroid

We use a Cartesian coordinate frame $\mathcal{F}(O; x_1, x_2, x_3)$ with $\widehat{\mathbf{e}}_1, \widehat{\mathbf{e}}_2$ denoting the dual unit vectors of the x_1- and x_2-axis. The axes $\widehat{\mathbf{p}}_{21}$ and $\widehat{\mathbf{p}}_{31}$ of the pinion Σ_2 and the gear Σ_3, respectively, are assumed to be symmetrically placed with respect to the x_1- and x_2-axes, as depicted in Fig. 3. Therefore,

$$
\begin{aligned}
\widehat{\mathbf{p}}_{21} &= \widehat{\mathbf{e}}_1 \cos\widehat{\alpha} - \widehat{\mathbf{e}}_2 \sin\widehat{\alpha} \\
\widehat{\mathbf{p}}_{31} &= \widehat{\mathbf{e}}_1 \cos\widehat{\alpha} + \widehat{\mathbf{e}}_2 \sin\widehat{\alpha} .
\end{aligned}
\tag{3}
$$

We limit ourselves to the skew case and assume

$$
0 < \alpha < \pi/2 \quad \text{and} \quad \alpha_0 \neq 0.
\tag{4}
$$

Let $\omega_{21}, \omega_{31} \in \mathbb{R}$ denote the angular velocities of the gears Σ_2 and Σ_3 with respect to the gear box Σ_1, respectively. Then, the screw $\widehat{\mathbf{q}}_{32}$ of the relative motion Σ_3/Σ_2 with axis $\widehat{\mathbf{p}}_{32}$ becomes

$$
\widehat{\mathbf{q}}_{32} = \widehat{\omega}_{32}\,\widehat{\mathbf{p}}_{32} = \widehat{\omega}_{32}\,(\widehat{\mathbf{e}}_1 \cos\widehat{\varphi} + \widehat{\mathbf{e}}_2 \sin\widehat{\varphi}) = \omega_{31}\,\widehat{\mathbf{p}}_{31} - \omega_{21}\,\widehat{\mathbf{p}}_{21}.
\tag{5}
$$

where $\widehat{\varphi} = \varphi + \varepsilon\varphi_0$ denotes the dual angle made by $\widehat{\mathbf{e}}_1$ and $\widehat{\mathbf{p}}_{32}$, as illustrated in Fig. 3. From eq. (4) the primal parts $\mathbf{p}_{31}$ and $\mathbf{p}_{21}$ are linearly independent. Hence, for any φ there is a choice of $(\omega_{21}, \omega_{31}) \in \mathbb{R}^2$, as per Fig. 5, where ω_{21}, ω_{31} and φ are shown as related by the primal part of eq. (5).

3

Comparing the coefficients of $\widehat{\mathbf{e}}_1$ and $\widehat{\mathbf{e}}_2$ reveals that eq. (5) is equivalent to

$$\begin{array}{rcl} \widehat{\omega}_{32}\cos\widehat{\varphi} &=& (\omega_{31}-\omega_{21})\cos\widehat{\alpha} \\ \widehat{\omega}_{32}\sin\widehat{\varphi} &=& (\omega_{31}+\omega_{21})\sin\widehat{\alpha}. \end{array} \qquad (6)$$

We eliminate $\widehat{\omega}_{32}$ by multiplying the two equations by $-\sin\widehat{\varphi}$ and by $\cos\widehat{\varphi}$, respectively, to obtain

$$\omega_{21}\sin(\widehat{\alpha}+\widehat{\varphi}) + \omega_{31}\sin(\widehat{\alpha}-\widehat{\varphi}) = 0, \qquad (7)$$

whose real coefficients are

$$\omega_{21} = -\lambda\sin(\alpha-\varphi), \quad \omega_{31} = \lambda\sin(\alpha+\varphi) \quad \text{for any } \lambda \in \mathbb{R}. \qquad (8)$$

The dual part of eq. (7) leads to

$$\omega_{21}(\alpha_0+\varphi_0)\cos(\alpha+\varphi) + \omega_{31}(\alpha_0-\varphi_0)\cos(\alpha-\varphi) = 0.$$

We replace the angular velocities ω_{i1} by functions of φ, as per eq. (8), thus obtaining

$$-(\alpha_0+\varphi_0)\sin(\alpha-\varphi)\cos(\alpha+\varphi) + (\alpha_0-\varphi_0)\sin(\alpha+\varphi)\cos(\alpha-\varphi) = 0$$

which can be rewritten as $-\alpha_0\sin 2\varphi + \varphi_0\sin 2\alpha = 0$. Hence, by setting

$$R = \frac{\alpha_0}{\sin 2\alpha} \qquad (9)$$

we obtain

$$\varphi_0 = \frac{\alpha_0}{\sin 2\alpha}\sin 2\varphi = R\sin 2\varphi, \qquad (10)$$

with φ_0 equal to the x_3-coordinate of the relative axis $\widehat{\mathbf{p}}_{32}$ — see Fig. 3 — thereby revealing that for a variable transmission ratio ω_{31}/ω_{21}, all relative axes are located on Plücker's conoid, which obeys

$$x_3 = 2R\,\sin\varphi\cos\varphi = 2R\,\frac{x_1 x_2}{x_1^2+x_2^2}, \qquad (11)$$

and is a cubic surface — see Fig. 4, cf. Figliolini and Angeles (2006). The distance $2R$ between the two torsal generators $\varphi = \pm\pi/4$ is called the *diameter* of the conoid.

On the other hand, we obtain from eqs. (6), after multiplying the two equations by $\cos\widehat{\varphi}$ and by $\sin\widehat{\varphi}$, respectively

$$\widehat{\omega}_{32} = \omega_{31}\cos(\widehat{\alpha}-\widehat{\varphi}) - \omega_{21}\cos(\widehat{\alpha}+\widehat{\varphi}). \qquad (12)$$

Using eq. (8), the primal part of eq. (12) yields, in turn,

$$\omega_{32} = \lambda\left[\sin(\alpha+\varphi)\cos(\alpha-\varphi) + \sin(\alpha-\varphi)\cos(\alpha+\varphi)\right] = \lambda\sin 2\alpha, \qquad (13)$$

the dual part of eq. (12) becoming

$$\begin{array}{rcl} \omega_{032} &=& -\omega_{31}(\alpha_0-\varphi_0)\sin(\alpha-\varphi) + \omega_{21}(\alpha_0+\varphi_0)\sin(\alpha+\varphi) \\ &=& \lambda\left[-(\alpha_0-\varphi_0)\sin(\alpha+\varphi)\sin(\alpha-\varphi) - (\alpha_0+\varphi_0)\sin(\alpha-\varphi)\sin(\alpha+\varphi)\right] \\ &=& -2\lambda\,\alpha_0\sin(\alpha+\varphi)\sin(\alpha-\varphi) = \lambda\,\alpha_0\,(\cos 2\alpha - \cos 2\varphi). \end{array}$$

Finally, we obtain the pitch h_{32} as

$$h_{32} = \frac{\omega_{032}}{\omega_{32}} = R(\cos 2\alpha - \cos 2\varphi). \tag{14}$$

Equations (10) and (14) are the basis of Disteli's diagram, which he disclosed in (Disteli, 1911, Fig. 2, p. 250), as displayed in Fig. 5.

Disteli's diagram illustrates the relation among the pitch h_{32}, the angle φ and the distance φ_0, with the velocities ω_{21} and ω_{31}.

Figure 5: Disteli's diagram

Figure 6: The Central Angle Theorem

The diagram is based on a projection in the direction of the common normal $\widehat{\mathbf{e}}_3$ between $\widehat{\mathbf{p}}_{21}$ and $\widehat{\mathbf{p}}_{31}$ — cf. Fig. 3. The projections $\widehat{\mathbf{p}}_{21}', \widehat{\mathbf{p}}_{31}'$ of the shafts intersect at point $3 = \widehat{\mathbf{e}}_3'$ at an angle 2α. The projection $\widehat{\mathbf{p}}_{32}'$ of the relative axis has the direction of the difference vector $\mathbf{p}_{32} = \omega_{31}\mathbf{p}_{31} - \omega_{21}\mathbf{p}_{21}$. We use a circle k which passes through $\widehat{\mathbf{e}}_3'$ such that the remaining points 1, 2 of intersection between k and the views $\widehat{\mathbf{p}}_{21}', \widehat{\mathbf{p}}_{31}'$ lie at a distance $2\alpha_0$.[2] Then, the remaining point 4 of intersection between k and $\widehat{\mathbf{p}}_{32}'$ shows the distance φ_0 and the corresponding pitch h_{32}. The diagram is a consequence of eqs. (10) and (14) and the Central Angle Theorem — see Fig. 6.

Remark. For any given φ the distance φ_0 can be derived with the aid of circle k. There is also a pure geometric explanation for this: Tangent planes τ intersect the Plücker conoid Ψ in a line and a conic c — see Fig. 4. The 'top view' in the direction of the double line $\widehat{\mathbf{e}}_3$ of Ψ maps the conic c onto a circle k, for a tangent plane τ with a 45° inclination — see Figs. 7 and 8. The line through an arbitrary point of k and parallel to the h_{32}-axis can be seen as the top view of a 'horizontal' line within τ. Because of the 45° inclination, the distance between any two such parallel lines equals the difference between the heigths of the corresponding points and generators of Ψ. More about the geometry of Plücker's conoid can be found in the section below.

---

[2] Because of the free choice of point $1 \in \widehat{\mathbf{p}}_{21}'$, there is still a continuum of possible circles k through $\widehat{\mathbf{e}}_3'$, of radius R.

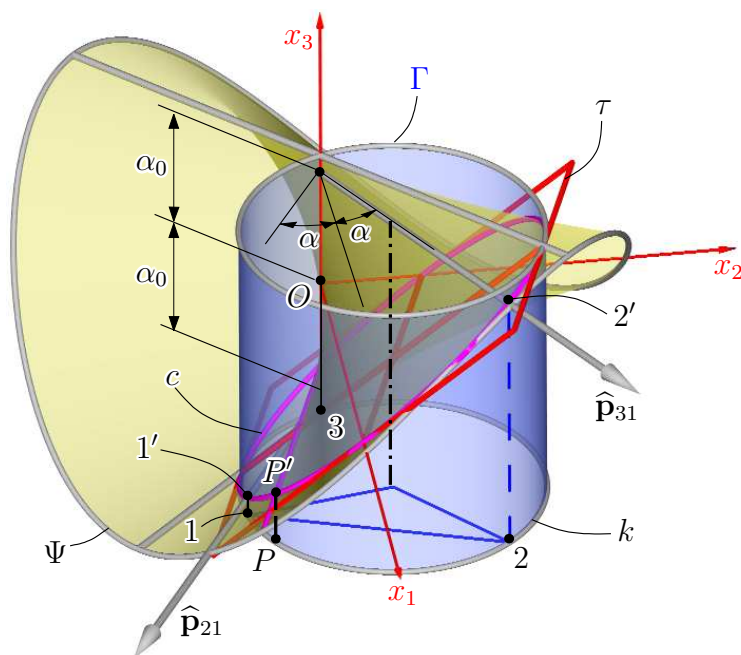## 2 Examples: Plücker's conoid and Disteli's Diagram

Figure 7: Three-Dimensional view of Disteli's diagram ($\alpha = 30°$, $\alpha_0 = 43.3\,\text{mm}$ and $R = 50\,\text{mm}$)

With reference to the case of Fig. 7, the skew axes $\widehat{\mathbf{p}}_{21}$ and $\widehat{\mathbf{p}}_{31}$ of the pinion Σ_2 and gear Σ_3, respectively, are assigned through the distance $\alpha_0 = 43.30\,\text{mm}$ and angle $\alpha = 30°$. Consequently, the half diameter R of the corresponding Plücker conoid Ψ is equal to $50\,\text{mm}$. Disteli's Diagram to analyze the relative screw motion between pinion and gear is obtained by referring to frame $\mathcal{F}(O; x_1, x_2, x_3)$, which shows: the origin O symmetrically located on the diameter of the conoid; the x_1-axis making an angle $\alpha = 30°$ with both axes $\widehat{\mathbf{p}}_{21}$ and $\widehat{\mathbf{p}}_{31}$, respectively; the x_3-axis directed along the diameter of the conoid; and, finally, the x_2-axis orthogonal to the x_1- and x_3-axes.

Thus, the circle k of Disteli's diagram is obtained by considering a cylinder Γ passing through the x_3-axis, which also means that the axis of the cylinder is parallel to the x_3-axis. Rotating this cylinder Γ of radius R about the x_3-axis while fixing the Plücker conoid Ψ yields a one-parameter set of intersection curves c between Γ and Ψ. Each curve c of this set is an ellipse. Moreover, the plane τ of the ellipse c is also a tangent plane to the Plücker conoid Ψ and shows always an inclination of $45°$ with respect to a horizontal plane, which is parallel to the x_1- and x_2-axes. The intersection between this plane and the Plücker conoid Ψ is given by the ellipse c and a line normal to x_3, because Ψ is a cubic surface. Of course, the tangent point P' between τ and Ψ changes according to the position of the cylinder Γ with respect to Ψ. Disteli's diagram is obtained by projecting the three-dimensional drawing on the horizontal plane, the position of points 1 and 2 on circle k depending on the particular position of the cylinder Γ with radius $R = 50\,\text{mm}$, which can be chosen arbitrarily.

Likewise, Disteli's diagram can be obtained by referring to the particular case of Fig. 8, where the skew axes $\widehat{\mathbf{p}}_{21}$ and $\widehat{\mathbf{p}}_{31}$ of the pinion Σ_2 and gear Σ_3, respectively, are assigned through the
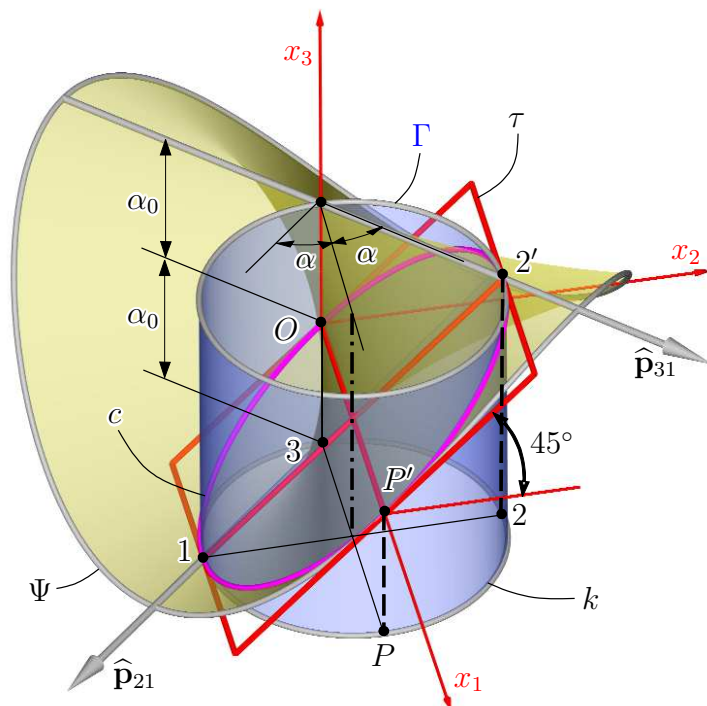
Figure 8: Three-Dimensional view of Disteli's Diagram ($\alpha = 45°$, $\alpha_0 = R = 50\,\text{mm}$)

distance $\alpha_0 = R = 50\,\text{mm}$ and the angle $\alpha_0 = 45°$, which means that $\widehat{\mathbf{p}}_{21}$ and $\widehat{\mathbf{p}}_{31}$ coincide with the torsal generators of the corresponding Plücker conoid Ψ.

In this particular case, the cylinder Γ can be chosen conveniently, with its axis intersecting the x_1-axis of frame $\mathcal{F}$. Consequently, plane τ of the ellipse c intersects the Plücker conoid Ψ along a line passing through the minor semi-axis of the ellipse c.

Moreover, referring to Fig. 8, the tangent point P' of the plane τ with Ψ is located on the x_1-axis a distance $2R$ from the x_3-axis, the inclination of $45°$ of plane τ with respect to the horizontal plane being also indicated.

3 Disteli's Diagram: General Case

Now we adress the more general case where the instantaneous motions of Σ_2 and Σ_3 with respect to Σ_1 are supposed to be helical, with dual angular velocities $\widehat{\omega}_{21}$ and $\widehat{\omega}_{31}$, respectively. We keep the pitches

$$h_{21} = \omega_{021}/\omega_{21} \quad \text{and} \quad h_{31} = \omega_{031}/\omega_{31} \tag{15}$$

constant, while the ratio ω_{21}/ω_{31} varies. It will be proven that the axes $\widehat{\mathbf{p}}_{32}$ of the relative motion Σ_3/Σ_2 again cover a Plücker conoid. There is again a diagram of the Disteli type. In (Disteli, 1914, Fig. 6, p. 295) a similar diagram is shown.

The dual analogue of eq. (7) reads

$$\widehat{\omega}_{21} \sin(\widehat{\alpha} + \widehat{\varphi}) + \widehat{\omega}_{31} \sin(\widehat{\alpha} - \widehat{\varphi}) = 0. \tag{16}$$

whose primal part remains unchanged, eq. (8) still holding. The dual part of eq. (16) gives

$$\omega_{021}\sin(\alpha+\varphi)+\omega_{21}(\alpha_0+\varphi_0)\cos(\alpha+\varphi)+\omega_{031}\sin(\alpha-\varphi)+\omega_{31}(\alpha_0-\varphi_0)\cos(\alpha-\varphi)=0$$

which can be expressed as

$$\omega_{21}\left[h_{21}\sin(\alpha+\varphi)+(\alpha_0+\varphi_0)\cos(\alpha+\varphi)\right]+\omega_{31}\left[h_{31}\sin(\alpha-\varphi)+(\alpha_0-\varphi_0)\cos(\alpha-\varphi)\right]=0.$$

Further, we substitute the angular velocities ω_{i1} by functions of φ, as per eq. (8), to obtain

$$\lambda\left[-h_{21}\sin(\alpha-\varphi)\sin(\alpha+\varphi)+h_{31}\sin(\alpha+\varphi)\sin(\alpha-\varphi)-\right.$$
$$\left.-(\alpha_0+\varphi_0)\sin(\alpha-\varphi)\cos(\alpha+\varphi)+(\alpha_0-\varphi_0)\sin(\alpha+\varphi)\cos(\alpha-\varphi)\right]=0$$

which can be rewritten as

$$\tfrac{1}{2}(h_{21}-h_{31})(\cos 2\alpha-\cos 2\varphi)+\alpha_0\sin 2\varphi-\varphi_0\sin 2\alpha=0,$$

hence, from eq. (9), as a generalization of eq. (10),

$$\varphi_0=R\sin 2\varphi+\frac{h_{21}-h_{31}}{2\sin 2\alpha}\left(\cos 2\alpha-\cos 2\varphi\right). \tag{17}$$

On the other hand, the dual analogue of eq. (12) reads

$$\widehat{\omega}_{32}=\widehat{\omega}_{31}\cos(\widehat{\alpha}-\widehat{\varphi})-\widehat{\omega}_{21}\cos(\widehat{\alpha}+\widehat{\varphi}). \tag{18}$$

The primal part of eq. (8), displayed in eq. (13), remains again unchanged. After substituting eqs. (15) and (8) into the dual part of eq. (18), we obtain

$$\begin{aligned}\omega_{032}&=\lambda\left[\sin(\alpha+\varphi)\left[h_{31}\cos(\alpha-\varphi)-(\alpha_0-\varphi_0)\sin(\alpha-\varphi)\right]+\right.\\&\left.+\sin(\alpha-\varphi)\left[h_{21}\cos(\alpha+\varphi)-(\alpha_0+\varphi_0)\sin(\alpha+\varphi)\right]\right]=\\&=\lambda\left[\tfrac{1}{2}h_{31}(\sin 2\alpha+\sin 2\varphi)+\tfrac{1}{2}h_{21}(\sin 2\alpha-\sin 2\varphi)+\alpha_0(\cos 2\alpha-\cos 2\varphi)\right].\end{aligned}$$

Hence the dual analogue of eq. (14) reads

$$h_{32}=\frac{\omega_{032}}{\omega_{32}}=\tfrac{1}{2}(h_{21}+h_{31})+\frac{h_{31}-h_{21}}{2\sin 2\alpha}\sin 2\varphi+R(\cos 2\alpha-\cos 2\varphi). \tag{19}$$

Upon setting

$$S=\frac{h_{31}-h_{21}}{2\sin 2\alpha}$$

we can summarize eqs. (17) and (19), namely,

$$\begin{aligned}\varphi_0&=S\cos 2\varphi+R\sin 2\varphi-S\cos 2\alpha,\\h_{32}&=S\sin 2\varphi-R\cos 2\varphi+R\cos 2\alpha+\tfrac{1}{2}(h_{31}+h_{21}).\end{aligned} \tag{20}$$

Next, we replace R and S by introducing two new constants, T and ψ, upon setting
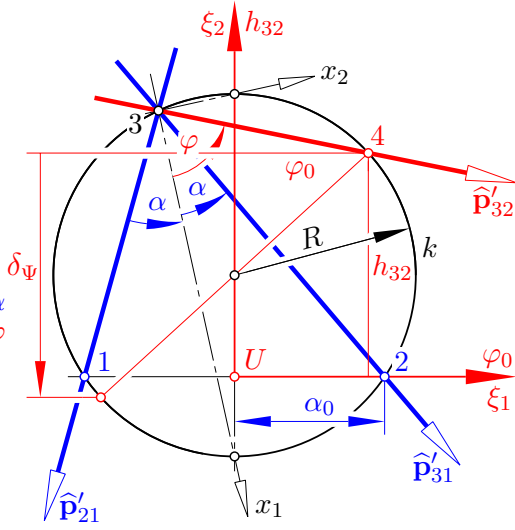
$$S=-T\sin\psi,\quad R=T\cos\psi. \tag{21}$$

Figure 9: General version of Disteli's diagram

Hence, eq. (20) takes the new form

$$
\begin{aligned}
\varphi_0 &= T\sin(2\varphi - \psi) + T\cos 2\alpha \sin\psi, \\
h_{32} &= -T\cos(2\varphi - \psi) + T\cos 2\alpha \cos\psi + \tfrac{1}{2}(h_{31} + h_{21}),
\end{aligned}
\tag{22}
$$

which proves that the relative axes $\widehat{\mathbf{p}}_{32}$ cover again a Plücker conoid, this time with diameter $2T = 2\sqrt{R^2 + S^2}$ — note the alternative short proof in (Pottmann and Wallner, 2001, pp. 179–180).

In order to draw the diagram of Fig. 9, we start with a free choice of the coordinate frame $\mathcal{F}(U; \xi_1, \xi_2)$. The two axes will later serve as the φ_0- and h_{32}-axis, respectively. Then, we draw the points 1 and 2 having coordinates $(\xi, \eta) = (-\alpha_0, h_{21})$ and $(-\alpha_0, h_{31})$, respectively. We determine the circle k through points 1 and 2 such that the central angle for the arc 12 is 4α. We may choose the point $3 \in k$ as the top view of the common perpendicular $\widehat{\mathbf{e}}_3$. Then, for any given angle φ, the remaining point 4 of intersection between $\widehat{\mathbf{p}}_{32}$ and k defines the corresponding φ_0 and the pitch h_{32}.

4 Distribution Parameters in Disteli's Diagram

The distribution parameter $\delta(t)$ of the ruled surface $\widehat{\mathbf{g}}(t) = \mathbf{g}(t) + \varepsilon\, \mathbf{g}_0(t)$ is given by

$$
\delta = \frac{\dot{\mathbf{g}} \cdot \dot{\mathbf{g}}_0}{\dot{\mathbf{g}} \cdot \dot{\mathbf{g}}}
\tag{23}
$$

according to (Stachel, 2000, Theorem 1). Parameter δ rules the distribution of tangent planes along any generator. The tangent planes at the points X in distance $\pm\delta$ to the striction point S make an angle of $\pm 45°$ with the tangent plane at S.

Figure 10: Distribution parameter
δ_Ψ of Plücker's conoid Ψ
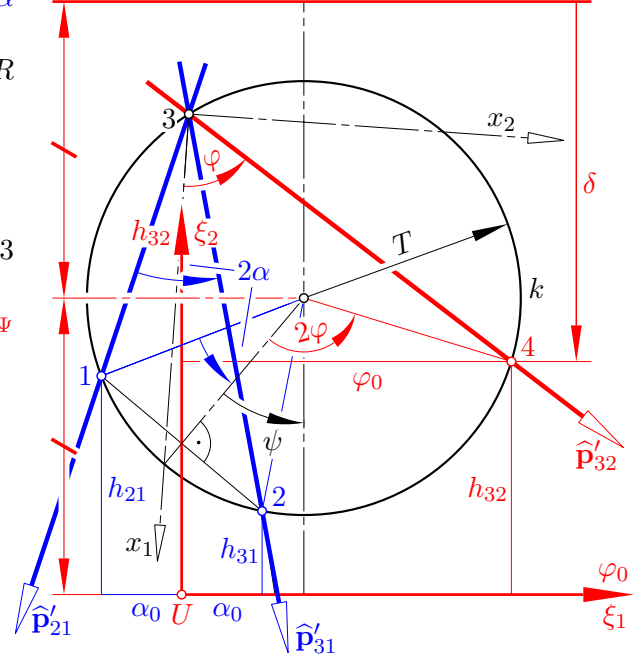
Figure 11: Distribution parameter
δ of the axodes of Σ_3/Σ_2

In order to compute the distribution parameter δ_Ψ of any generator $\widehat{\mathbf{g}} = \widehat{\mathbf{p}}_{32}$ of Plücker's conoid Ψ, we use the representation in eqs. (5) and (10):

$$\widehat{\mathbf{g}} = (\cos\varphi - \varepsilon\varphi_0\sin\varphi)\widehat{\mathbf{e}}_1 + (\sin\varphi + \varepsilon\varphi_0\cos\varphi)\widehat{\mathbf{e}}_2 \quad \text{with} \quad \varphi_0 = R\sin 2\varphi.$$

Differentiation with respect to the (real) parameter φ gives

$$\dot{\widehat{\mathbf{g}}} = (-\sin\varphi - \varepsilon\varphi_0\cos\varphi - 2\varepsilon R\sin\varphi\cos 2\varphi)\widehat{\mathbf{e}}_1 + (\cos\varphi - \varepsilon\varphi_0\sin\varphi + 2\varepsilon R\cos\varphi\cos 2\varphi)\widehat{\mathbf{e}}_2.$$

The equations $\widehat{\mathbf{e}}_1\cdot\widehat{\mathbf{e}}_1 = 1$ and $\widehat{\mathbf{e}}_1\cdot\widehat{\mathbf{e}}_2 = 0$ imply

$$\begin{aligned}
\dot{\widehat{\mathbf{g}}}\cdot\dot{\widehat{\mathbf{g}}} &= (-\sin\widehat{\varphi} - 2\varepsilon R\sin\varphi\cos 2\varphi)^2 + (\cos\widehat{\varphi} + 2\varepsilon R\cos\varphi\cos 2\varphi)^2 = \\
&= 1 + 4\varepsilon R\cos 2\varphi = \dot{\mathbf{g}}\cdot\dot{\mathbf{g}} + 2\varepsilon\,\dot{\mathbf{g}}\cdot\dot{\mathbf{g}}_0.
\end{aligned}$$

Following eq. (23), we use the dual and the primal part of $\dot{\widehat{\mathbf{g}}}\cdot\dot{\widehat{\mathbf{g}}}$ to obtain

$$\delta_\Psi = 2R\cos 2\varphi. \tag{24}$$

Figure 10 shows where δ_Ψ is included in Disteli's diagram for the special case — as per Section 1. All striction points of Plücker's conoid Ψ are located on the x_3-axis of our coordinate frame, while the corresponding tangent planes are vertical, as noted in Figs. 7 and 8. Therefore, if the tangent plane τ of Ψ at any point P' has a 45° inclination with the horizontal x_1-x_2-plane, then the perpendicular distance between P' and the x_3-axis equals the distribution parameter δ_Ψ of the generator $\widehat{\mathbf{g}}$ passing through P'.

Now we recall the general case treated in Section 3: Let $\widehat{\mathbf{p}}_{32}$ be the *instant screw axis* of the relative motion between the two frames Σ_2 and Σ_3. Moreover, we assume that the axes $\widehat{\mathbf{p}}_{21}$ and $\widehat{\mathbf{p}}_{31}$ are fixed in the gear box Σ_1. Then, for constant $\widehat{\omega}_{21}$ and $\widehat{\omega}_{31}$, the relative axis $\widehat{\mathbf{p}}_{32}$ remains also fixed in the gear box Σ_1. However, with respect to Σ_2 and Σ_3 the relative axis $\widehat{\mathbf{p}}_{32}$ traces the axodes of the relative motion Σ_3/Σ_2. In the case of *bevel gears*, moving under pure rotation, $\widehat{\omega}_{21}, \widehat{\omega}_{31} \in \mathbb{R}$ — as per Section 1 — the axodes are hyperboloids; otherwise — Section 3 — ruled helical surfaces. We want to prove that the distribution parameter δ, which is constant for each axode and shared by both, can also be viewed in Disteli's diagram:

The axode in Σ_2 is traced by $\widehat{\mathbf{g}} = \widehat{\mathbf{p}}_{32}$ under the helical motion Σ_1/Σ_2 with the instantaneous screw $-\widehat{\omega}_{21}\,\widehat{\mathbf{p}}_{21}$. The dual analogue of eq. (5), namely,

$$\widehat{\omega}_{32}\,\widehat{\mathbf{g}} = \widehat{\omega}_{31}\,\widehat{\mathbf{p}}_{31} - \widehat{\omega}_{21}\,\widehat{\mathbf{p}}_{21}$$

leads, with (Stachel, 2000, eq. (9)), to the derivative $\dot{\widehat{\mathbf{g}}} = -\widehat{\omega}_{21}\,\widehat{\mathbf{p}}_{21} \times \widehat{\mathbf{g}}$, i.e.,

$$\begin{aligned}
\widehat{\omega}_{32}\,\dot{\widehat{\mathbf{g}}} &= -\widehat{\omega}_{21}\,\widehat{\mathbf{p}}_{21} \times (\widehat{\omega}_{31}\,\widehat{\mathbf{p}}_{31} - \widehat{\omega}_{21}\,\widehat{\mathbf{p}}_{21}) = \\
&= -\widehat{\omega}_{21}\,\widehat{\omega}_{31}(\widehat{\mathbf{p}}_{21} \times \widehat{\mathbf{p}}_{31}) = -\widehat{\omega}_{21}\,\widehat{\omega}_{31}\sin 2\widehat{\alpha}\,\widehat{\mathbf{e}}_3
\end{aligned}$$

according to eq. (1) and Fig. 3. In order to compute the distribution parameter we again need the primal and the dual part of

$$\widehat{\omega}_{32}^2\,\dot{\widehat{\mathbf{g}}}{\cdot}\dot{\widehat{\mathbf{g}}} = \widehat{\omega}_{21}^2\,\widehat{\omega}_{31}^2\sin^2 2\widehat{\alpha}\,.$$

Under the condition $\omega_{32} \neq 0$, the inverse of $\widehat{\omega}_{32}^2$ exists, and we obtain, as per eq. (15),

$$\dot{\widehat{\mathbf{g}}}{\cdot}\dot{\widehat{\mathbf{g}}} = \frac{\omega_{21}^2\omega_{31}^2\sin 2\alpha}{\omega_{32}^2}(1 + 2\varepsilon h_{21})(1 + 2\varepsilon h_{31})(1 - 2\varepsilon h_{32})(\sin 2\alpha + 4\varepsilon\,\alpha_0\cos 2\alpha).$$

Following eq. (23) the distribution parameter of the axodes reads

$$\delta = h_{21} + h_{31} - h_{32} + 2R\cos 2\alpha = R\cos 2\varphi + \tfrac{1}{2}(h_{31} + h_{21}) - S\sin 2\varphi + R\cos 2\alpha$$

due to the second equation in (20). Finally, we replace R and S by T and ψ, according to eq. (21), thereby ending up with the formula

$$\delta = T\cos(2\varphi - \psi) + T\cos 2\alpha\cos\psi + \tfrac{1}{2}(h_{31} + h_{21}). \tag{25}$$

for the distribution parameter of the axodes of the relative motion Σ_3/Σ_2. Shown in Fig. 11 is how δ can be figured out from the same diagram used in Fig. 9 to obtain the position and the pitch of the relative motion.

Conclusions

The Disteli's diagram has been analyzed and proposed in a new form. This diagram can find several applications to analyze the relative screw motion between two rigid bodies, which are moving according to a general helical motion. However, particular attention has been devoted to the case of skew gears. Some examples are also reported.

References

J. Angeles. The application of dual algebra to kinematic analysis. In J. Angeles, E. Zakhariev (eds.): *Computational Methods in Mechanical Systems*, volume 161, pages 3–31, Heidelberg, 1998. Springer-Verlag.

W. K. Clifford. Preliminary sketch of bi-quaternions. *Proc. London Math. Soc.*, 4(64, 65): 381–395, 1873.

W. K. Clifford. *Mathematical Papers* (ed. by R. Tucker). MacMillan and Co., London, 1882.

M. Disteli. Über instantane Schraubengeschwindigkeiten und die Verzahnung der Hyperboloidräder. *Z. Math. Phys.*, 51:51–88, 1904.

M. Disteli. Über die Verzahnung der Hyperboloidräder mit geradlinigem Eingriff. *Z. Math. Phys.*, 59:244–298, 1911.

M. Disteli. Über das Analogon der Savaryschen Formel und Konstruktion in der kinematischen Geometrie des Raumes. *Z. Math. Phys.*, 62:261–309, 1914.

G. Figliolini and J. Angeles. The synthesis of the pitch surfaces of internal and external skew-gears and their racks. *ASME Journal of Mechanical Design*, 2006. to appear.

M. Husty, A. Karger, H. Sachs, and W. Steinhilper. *Kinematik und Robotik*. Springer-Verlag, Berlin, Heidelberg, 1997.

J. M. McCarthy. *Geometric Design of Linkages*. Springer-Verlag, New York, 2000.

H. R. Müller. *Kinematik*. Sammlung Göschen, Walter de Gruyter, Berlin, 1963.

H. Pottmann and J. Wallner. *Computational Line Geometry*. Springer-Verlag, Berlin, Heidelberg, 2001.

F. Schur. Nachruf auf Martin Disteli. *Jahresber. Deutsch. Math.-Verein.*, 36:170–173, 1927.

H. Stachel. Instantaneous spatial kinematics and the invariants of the axodes. In *Proc. Ball 2000 Symposium*, number 23, Cambridge, 2000.

H. Stachel. Teaching spatial kinematics for engineers. In *Proceedings ICEE 2005*, volume 2, pages 845–851, Gliwice, Poland, 2005.

G. R. Veldkamp. On the use of dual numbers, vectors, and matrices in instantaneous spatial kinematics. *Mech. and Mach. Theory*, 11:141–156, 1976.